Electrically Enhanced Harvesting of Water Vapor from the Air

Michael Reznikov, Matthew Salazar, Martin Lopez
Physical Optics Corp.
phone: (1)310-320-3088
contact e-mail: mreznikov@poc.com

Melixa Rivera-Sustache
ERDEC-CERL
phone: (1)217-373-3477

***Abstract*— The global consumption of potable water has increased six-fold over the past century. As a result, the demand for drinkable water is very high: 1.2 billion people in this world do not have access to drinking water and 2.4 billion have no adequate sanitation. Existing state-of-the-art "atmospheric water generation" (AWG) systems consume amounts of energy per liter of water provided that are very similar to those of imported bottled water in small single-use plastic containers. Therefore, any technology that generates usable water in an energy-efficient manner is required. A bench-top prototype of a new Moisture Harvester (MOHA) technology was built and evaluated. The MOHA system utilizes electrostatic enhancement of phase-change processes such as the nucleation of water vapor (moisture) in the airflow and improved heat exchange during condensation. The main advantage of MOHA technology is the energy-efficient harvesting of water from the airstream due to the selective electrostatic extraction of moisture from the air and electrospray enhanced condensation of water. Experiments carried with the 1:613 scale prototype (compared to the pilot-scale system) demonstrated an ~7.5 mL/hr water harvesting rate (~ 1.2 gal/hr in full scale) at reduced cooling power (11W) applied to the condenser. The same prototype without the electrostatic enhancement harvested water at the rate -1.5 mL/hr, i.e. the five-fold improvement is experimentally demonstrated.**

I. Introduction

Drawing water from air (a so called atmospheric water generation, AWG) is a generic technology that produces potable water from water vapor in the air by a process that is a kind of dehumidification: difference is only in the product fluid, dehumidified air or the condensed humidity. The basic approach is to cool the atmospheric air below its dew point temperature, i.e. extract the specific heat of humid air and then the latent heat in the water content, and water begins to condense. In fact, this approach, if utilizing the day/night temperature difference, is known from ancient times as dew wells or dew ponds. There are two opportunities for electrostatics to improve this process: (a) to decrease the energy consumption by the minimizing the parasitic cooling of air; and (b) to increase the

condensation rate by the enhancing of water delivery to the cooling surface by the external field.

We have reported before [1,2] that the ionization of air allows for ~16 - 20% dehumidification due to the dielectrophoretic nucleation of polar water molecules on ions. The ionization approach has the inherent restraint due to the limited charge of ion, which serves as a nucleation center. In turn, the equilibrium size of liquid phase (micro-droplets) is restricted and the equilibrium vapor pressure (the residual vapor pressure in case of dehumidification) is correspondingly elevated. However, if electrospray droplets serve as nucleation centers, they are mostly charged to 80-85% of the Rayleigh limit when electrostatic forces do not exceed those of surface tension. As a result, the size of micro-droplets increases [3]. The bonus advantage of the electrospray is the direct deposition of liquid phase onto the cooling wall that minimizes the energy consumption for the cooling of air. We have demonstrated the 57% improvement of condensation rate for the condensation of steam [3]. Of course, the effect of electrospray varies from 50% (if there is very hot ambient temperature and insufficient power is handled by the cooling system) to nothing in the cold environment and with the powerful cooling system.

In short words, the electrostatic enhancement of condensation is based on the combination of three phenomena:

1) the dielectrophoretic (DEP) nucleation of the vapor on electrically charged centers;

2) the electrohydrodynamic (EHD) flow of the vapor due to the drag by electrically charged droplets; and

3) the temporal (until droplets are discharged) storage of heat energy in electrically charged droplets.

This work, which was supported by U.S. Army Corps of Engineers, addresses the water harvesting from the relatively humid (~ 80% RH) air exhausting from vented facility (shower room, kitchen, laundry etc.). Nevertheless, the results of this work are directly applicable to the atmospheric water harvesting. For example, the relative humidity in Mojave Desert rises from 25% during the daytime to 50% at night due to the natural cooling of air. Of course, the power consumption by fans will increase because the higher volume of air should be processed.

II. Brief Theoretical Background

A. Effect of Corona Discharge

When a water molecule is placed in a gradient electric field of magnitude E, such a polar molecule experiences DEP force $F_{dp} = \rho_o \mathrm{grad} E$ is directed to the side of the increased field E, i.e. toward the electrically charged center of nucleation. This produces a gradient of the vapor concentration and the steady state occurs when the DEP drift and the local diffusion flows are equal, which leads to the classic Maxwell distribution of the vapor concentration, i.e., $n(r_0) = n_\infty \exp(U(r_0)/kT)$, where k is Boltzmann's constant, T is the absolute temperature, and the potential energy of a molecule at distance r_0 from point charge q is $U(r_0)$. This energy can be calculated by the integration of the DEP force from distance r_0 to infinity as follows:

$$U = \rho_0 \int_{r_0}^{\infty} gradEdr = \rho_0 q / (4\pi\varepsilon_0 r_0^{\,2}) . \qquad (1)$$

If the additional potential energy due to the drift of dipoles as in Eq. (1) is accounted for, the classic Kelvin-Thomson equation for the saturated vapor pressure, p^{β} near the surface of a drop with radius R

$$p_C^{\beta} = p_{\infty} \exp[\frac{2\gamma v^l}{kTR} - \frac{q^2 v^l}{32\pi^2 kT\varepsilon_0 R^4}(\frac{1}{\varepsilon^{\beta}} - \frac{1}{\varepsilon^l})], \qquad (2)$$

where v^i is a volume per single molecule in liquid, and p_{∞} is the pressure of saturated water vapor above a flat surface at temperature T, is modified to

$$p_M^{\beta} = p_C^{\beta} \exp[-\frac{\rho_0 q}{4\pi kTR^2}] . \qquad (3)$$

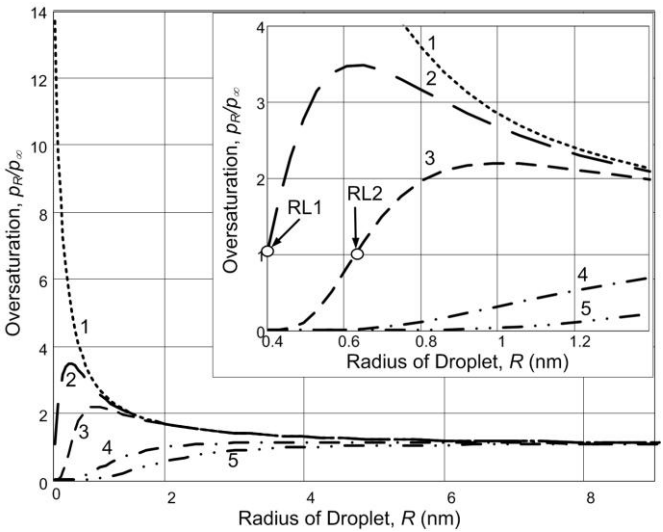

Fig. 1. Oversaturation of vapor pressure near the droplet of radius R, p_R, relative to the saturated vapor pressure over the flat surface of water, p_∞, that illustrates the effect of electric charge: 1 = neutral droplet; 2 and 3 = droplets with single and double electron charges, correspondingly, according to the classic Kelvin-Thomson equation (2); 4 and 5 = droplets with single and double electron charges respectively, according to the modified Kelvin-Thomson equation (3). Circles show the Rayleigh limits when droplet disintegrates due to electrical forces.

Thus the charged droplet acquires additional negative potential energy, which may be interpreted either as increased latent heat of evaporation or decreased effective surface tension in the basic Kelvin equation $p^{\beta} = p_{\infty} \exp(2\gamma v^l / kTR)$.

B. Effect of Electrospray

The dielectrophoretic potential of vapor molecules near the surface of charged droplet increases proportionally to the charge in the droplet and correspondingly adds to the latent heat for evaporation of this droplet. Fig. 2 illustrates that this increment in the evaporation energy is significant only for small, <10 μm, droplets, but the total latent heat for evaporation of these droplets is relatively small. As a result, the dielectrophoretic potential notably affects the stability of small droplets only.

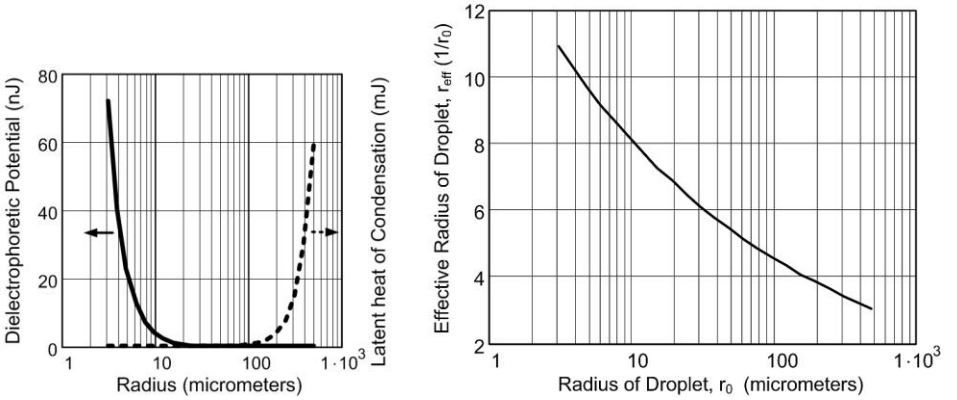

(a) (b)

Fig. 2. Effect of droplets charged to the Rayleigh limit: (a) - Dielectrophoretic potential of a droplet (solid line, left vertical axis) compared with the latent heat evaporation of this droplet (dotted line, right vertical axis). Note that the dielectrophoretic potential reaches a significant magnitude for a small, <10 μm, droplet, while the latent heat of condensation notably increases for larger droplets; (b) - Effective vapor collection radius, which is related to the distance where the dielectrophoretic force creates the centripetal flow of vapor. Note that the effective radius of vapor collection is presented relatively to the actual radius of droplet.

C. Thermodynamics of charged droplet.

Equations (2) and (3) are related to the equilibrium of a water droplet of radius R with vapor. At this condition, the chemical potential of the molecule in the neutral droplet, $\mu^l(R,T)$, is equal to the chemical potential of a gas phase (vapor) water molecule near the surface of this droplet

$$\mu^{\beta}(R,T) = \mu^{0}(T) + kT\ln(p_{\infty}) + \frac{2\gamma v^{l}}{kTR}, \tag{4}$$

where $\mu^0(T)$ is the standard chemical potential of vapor, and p_∞ is the ambient vapor pressure. The modified Kelvin-Thomson equation is directly derived from

$$\mu^{\beta}(R,T,q) = \mu^{\beta}(R,T) - \Delta\mu_{DEP}, \tag{5}$$

where $\Delta\mu_{DEP} = \frac{q^2 v^l}{32\pi^2\varepsilon_0 R^4} + \frac{q\rho_0}{4\pi\varepsilon_0 R^2}$ is the decrement of chemical potential due to dielectrophoretic forces. We are neglecting here the impact of vapor polarization

$\Delta\rho_0(r) = \alpha E(r)$ due to the low polarizability of water molecules, α, and the relatively low electric field. The polarization of vapor as a dielectric shell (Born energy) $\Delta\mu_{pol}^{\beta} = q^2 / 8\pi\varepsilon^{\beta}\varepsilon_0 R$ was also neglected because it is ~10^{-20} J for R = 10 nm and a single electron charge, $q = e = 1.6\cdot10^{-19}$ C, while the dielectrophoretic contribution to the chemical potential is ~ $0.9\cdot10^{-12}$ J under same conditions.

The outcome from Eq. (5) is that the heat capacitance of the charged droplet is decreased. Indeed, at a constant droplet volume of $4\pi R^3/3$, the heat capacitance is proportional to the second derivative of Gibbs energy, $G = N\cdot\mu^{l}$, where N is the number of molecules in the cluster (droplet), and the chemical potential in the liquid, μ^{l}, is defined by Eq. (5). Therefore, the isochoric heat capacitance of the droplet is defined as

$$C_{V,N} = -T\left(\frac{\partial^2 G}{\partial T^2}\right)_{V,N} = -T\cdot N\left(\frac{\partial^2(\mu_n - \Delta\mu_{DEP})}{\partial T^2}\right)_V, \qquad (6)$$

where μ_n is the chemical potential in the neutral droplet according to Eq. (4). Therefore, the electric charge should decrease the heat capacitance of the droplet. This speculative conclusion is supported by experimental data from [4] where the effect of electric charge on $C_{V,N}$ was investigated by the measuring the evaporation rate of charged clusters. Fig. 6 presents results of this work for positively charged pure water clusters and water clusters formed on negative ions (O_2), (CO_3), or (NO_3). On other hand, the enthalpy of the charged droplet is higher than that of the same number of molecules in bulk neutral water. The excess enthalpy is stored as energy of electric polarization. This is supported by numerical modeling and experimental data [5].

In the context of electrostatic enhancement of condensation, the decrement of heat capacitance of electrically charged droplet means that the temperature of droplet decreases at the discharge on the grounded condensing wall. In other words, electrostatic energy partially replaces the latent heat of condensation during the nucleation on the charged nuclei that reduces the thermal load on the heat pump (refrigerator).

III. Experiment

A. Experimental Setup.

The experimental setup (see Fig. 3a) implements a thermoelectric cold plate cooler, CP-065 (TE Technology, Inc., Traverse City, MI), which provides cooling power up to 65 W while consuming up to 5.5 A of 24 VDC.

The evaluated system consists of two main stages — the moisture separator and the water condenser. The moisture separator, shown in Fig. 49(a), uses corona discharge, directed across the airflow. The nucleation of water molecules on the corona discharge ionized air leads to the creation of tiny, ~10 nm, microdroplets on ions. Due to the electrical charge, these droplets are moved across the airstream to the accelerating grid and thus separated from the main air flow. This concentrated moist air (actually fog) is supplied to the condenser shown in Fig. 3(b).

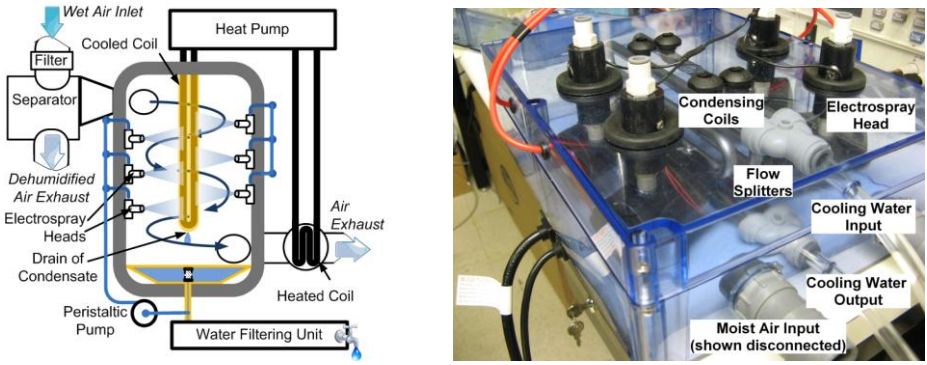

(a) (b)

Fig. 3. Experimental setup for evaluation of electrically enhanced harvesting of water vapor from the air: (a) - Scheme of setup; (b) The close look of electrically enhanced condenser.

The initial cylindrical position of the grounded electrode mesh in the vapor separator, which appears to be the optimal solution for the maximal drag flow, was rejected after the testing due to the high probability of sparks in the humid air. The physical reason for this corona instability in the humid air is the intensive nucleation of microscopic, nanoliter-size, charged droplets on corona-generated ions. While this nucleation is a moving force for moisture concentration, the decreased mobility of hydrated ions results in the increased electric field in the drift region of the corona discharge. At the given distance between electrodes, the probability of streamer discharges is elevated. To eliminate this problem, the cylindrical mesh electrodes were replaced by the flat mesh disks inserted in the branches of the cross-tree case.

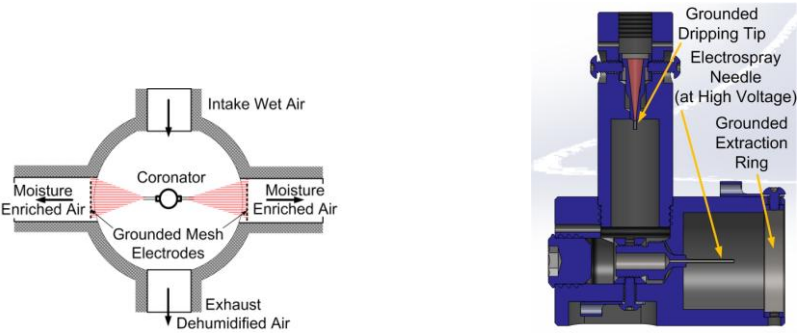

(a) (b)

Fig. 4. Schemes of main electrostatic components: (a) - moisture separator; (b) – electrospray emitter.

The core component of the electrically enhanced condenser is the array of electrospray heads (Fig. 4(b)). This head implements the double-stage design, which we developed previously for the steam condenser [3]. Each head contains the grounded electrostatic dripper tip, which supplies the liquid to electrospray needle (emitter) at the high voltage. The electrospray is stabilized by the grounded extraction ring in front of the needle. This

results in the stable electrospray invariably on the distance to the condensing wall and humidity of the air. The deposition of electrically sprayed liquid on the extraction ring is minimized by the design where the distance from the needle tip to the front plane of extraction ring is a~ ¾ of ring's internal radius.

The electrospray across the airflow in the condenser works like a wiper for humidity — the moisture is collected and delivered to the cooled coil, which extracts the latent heat without the necessity to cool the airstream. The heat exchange with the condensed water is provided by the stainless steel heat exchangers, LC-SSX1 from the same vendor (TE Technology, Inc.) as the CP-065 heat pump.

B. Experimental Data

The power supplied to the evaluated bench-scale prototype during the tests was monitored and kept stable during all tests. These parameters are presented in Table 1. The total power supplied to the prototype was ~78 W in the full power regime and ~21 W in the reduced power regime. In fact, the main power consumption (as seen in Table 1) is related to the thermoelectric chiller. The reason for this is that the cold plate cooler used, CP-065, provides 65 W of cooling power at full applied power, which is excessive for the evaluated prototype. As later tests demonstrated, this cooling power may be reduced to 14 W without notable effect on the water vapor harvesting rate at the extended surface of cooling coils.

TABLE 1: POWER CONSUMED BY BENCH-SCALE PROTOTYPE

Component	**Power Supplied, W**	**Notes**
Main fan	0.318/0.344	Corresponds to flow rate 0.43/1.63 cfm
Water circulation pump	3.75	
Water chiller, full power/reduced power	73.2/15.9	Corresponds to the cooling power of 65/14 W
Coronator	0.24	
Electrospray (four heads)	0.9	

Temperature and humidity sensors (THSs) are positioned in the evaluation setup as shown in Fig. 5.

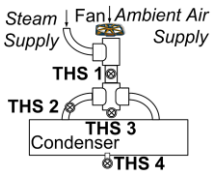

Fig. 5. Placement of temperature and humidity sensors (THSs) in the evaluation setup.

The utilization of these sensors is as follows:

THS 1 – Temperature and humidity of air/steam mixture BEFORE the 1st stage (moisture concentrator).
THS 2 – Temperature and humidity of air/steam mixture AFTER the 1st stage (moisture concentrator).
THS 3 – Temperature and humidity of main exhaust air.
THS 4 – Temperature and humidity of exhaust air from the condenser

Knowing the temperature and relative humidity of supplied and exhausting air through THS 1 and THS 2 as well the airflow, we were able to measure the percent of moisture extraction. THS 3 was used for the detection of moisture nucleation on a corona ion because this content of humidity, which is converted to the liquid phase, is excluded from measured relative humidity, which is related to the vapor phase only.

First, the bench-scale prototype was tested at full cooling power (65 W) in the chiller and elevated airflow at the intake. The goal of this test was to reveal the efficiency of moisture separator and effect of electrospray in the condenser. Distribution of airflow, absolute moisture content, and corresponding moisture flow between control points is presented in Table 2.

TABLE 2: TYPICAL VARIATION OF MOISTURE CONTENT AT MONITORING POINTS (SEE FIG. 5) AT FULL COOLING POWER (65 W)

Test point	**1**	**2**	**3**	**4**
Airflow, m^3/s	0.00077	0.00041	0.00059	0.00018
Airflow, cfm	1.63	0.87	1.25	0.38
Absolute moisture content, g/kg of dry air	16.1	16.8	15.7	8.8
Variation of moisture content from intake airflow, %	-	4.17	-2.4	-45
Absolute moisture flow, mg/s	14.9	3.64	11.1	1.91

Analysis of the data presented in Table 2 shows the following:

1. The absolute moisture flow (14.9 mg/s) is split in the single-stage separator into 3.64 mg/s (24.4%) to the condenser and 11.1 mg/s vented.
2. The measured humidity content of moisture in the air is enriched by ~4.2% after the separator, while the depletions of humidity after the separator and condenser are 2.4% and 45% respectively. This measured relative humidity of air corre-

sponds to the vapor phase only, while absolute moisture separation (24.4%) includes liquid water droplet phase, which is condensed on corona-created ions.

3. The condenser harvests moisture at a rate of 1.73 mg/s (47.5% of the incoming moisture flow), which corresponds to water vapor harvesting of 49.8 mL/day in an 8 hr test.

The actual amount of collected water vapor collected in 8 hr was 47 mL (total 517 mL minus 470 mL injected by the electrospray heads). The difference between the actual (47 mL) and calculated (49.8 mL) amounts may be attributed to the water left on the walls of the condensing chamber (2.8 mL).

To reveal the efficiency of the bench-scale prototype, we carried out a comparative series of tests. For this purpose we ran the prototype in three regimes: (1) Full system (all components ON); (2) Electrospray OFF with corona separator and cooler ON; and (3) Both electrospray and corona separator OFF, cooling system ON. Results of these tests are presented in Table 3. Please note that the moisture content was calculated according to data from the relative humidity sensor, which does not account for the liquid phase (mist droplets). The percent of moisture harvesting was defined by the change of moisture content. Tests were carried out at full cooling power (65 W).

TABLE 3: COMPARATIVE TESTS OF A PROTOTYPE AT FULL COOLING POWER (65 W)

Regime	**Condensate Collected, mL/hr**	**Absolute Moisture Content at the Intake, g/m^3**	**Absolute Moisture Content after the Separator, g/m^3**	**Absolute Moisture Content at the Exhaust of Condenser, g/m^3**
1	7.5	21.1	20.46	11.65
2	7.5	19.01	19.93	10.99
3	5.5	19.6	20.83	12.31

This test indicated that: (1) The moisture harvesting rate increased by 36% due to the electrostatic enhancement; (2) The residual moisture content is practically equal in all regimes, because it corresponds to the same temperature of the cooling coil (18°C); and (3). The moisture extraction from the intake airflow is improved by 20% due to the electrostatic enhancement. Only small differences in the improvement of the harvesting rate (2.5%) should be attributed to the effect of electrospray because the applied cooling power was excessive, which diminishes the effect of electrospray, as we demonstrated before [3]. In other words, the electrospray improves the performance of the condenser if there is a bottleneck in vapor delivery to the condensing wall. If the cooling power is excessive

and there is a high gradient of vapor density toward the condensing surface, there is no room for improvement.

Then we evaluated the prototype with lowered cooling power (11 W) as presented in Table 4.

TABLE 4: COMPARATIVE TESTS OF A PROTOTYPE AT LOW COOLING POWER (14 W)

Regime	**Condensate Collected, mL/hr**	**Absolute Moisture Content at the Intake, g/m^3**	**Absolute Moisture Content after the Separator, g/m^3**	**Absolute Moisture Content at the Exhaust of the Condenser, g/m^3**
Full system	7.5	20.3	16.4	13.4
W/o electrospray	1.5	20.3	15.8	13.8

This comparative test clearly demonstrated that the electrospray dramatically, by 5 times, improves the water vapor harvesting rate if the cooling power is reduced to 14 W and correspondingly the temperature of condensing coil increased to 22°C. At the same time, the measured residual moisture content increased by only 3% because the measured humidity content does not include the aerosol, liquid phase content.

A collected water was tested for total dissolved solids (TDS) content, total organic carbon (TOC) content, and total heterotrophic bacteria (total Coli, TC) content by a certified lab, EMAX Inc. Results of these tests are presented in Table 5.

TABLE 5: RESULTS OF TESTS FOR WATER SAMPLES COLLECTED BY THE BENCH-SCALE PROTOTYPE

Test	**Requirement**	**Test Result**
TDS	<500 mg/L	<20 mg/L
TOC	<0.5 mg/L	8.4 mg/L
TC	<1 CFU/100 mL	Absent

Results presented in Table 5 show that the product water was distilled (low TDS) and free from bacteria (low TC). The requirement for total organic carbon (TOC) exceeded the required level due to the intensive use of polymer materials and oil-lubricated valves in the bench-scale prototype to allow for fast modification. This problem may be easy eliminated in the real-scale system by use of a welded stainless-steel condenser with Teflon® isolators for electrospray emitters.

IV. Conclusion

The feasibility of evaluated concept for the electrostatic enhancement of water vapor harvesting from the air is experimentally proved. The five-fold improvement of the water collection rate with the improvised, non-optimized prototype is demonstrated.
Due to the limited performance of single-stage vapor separator, 24.4% of incoming humidity content, the further improvement of performance is possible by the using of multistage separator as shown in Fig. 6(a). Fig. 6(b) shows how the percentage of separated humidity increases with the number of separating stages at the airflow split and that the residual moisture flow (the moisture content not captured by the separator) decreases when the number of stages is increased, while the moisture flow, which is not processed (not captured) in the condenser, increases because the efficiency of the condenser was not varied in this simulation. Therefore, the implementation of a multistage separator requires an increment of heat-exchange surface area in the condenser to capture the maximal amount of the separated moisture.

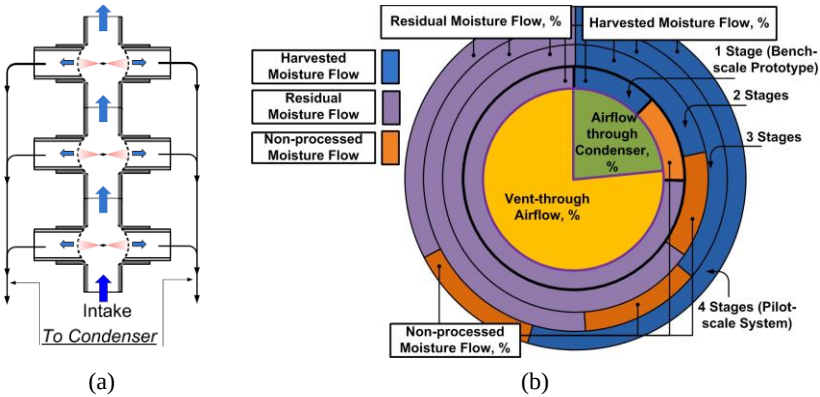

(a) (b)

Fig. 5. Effect of multistage moisture separator: (a) The example of a multistage separator design; (b) The improvement of moisture harvesting flow with varying numbers of stages in separator. The central circle in the diagram shows the constant split of airflow in the system..

References

[1] M. Reznikov, "Dielectrophoretic Dehumidification of Gas Stream in Low and Moderate Electrical Fields," *Proc. ESA-IEEE Joint Meeting of Electrostatics, Little Rock, AR*, June 24 27, 2003, pp. 230-240.

[2] M. Reznikov, "Electrically Enhanced Condensation I: Effects of Corona Disch*arge," IEEE Trans. Industry Applications*, vol. 51, no. 2, 2015, pp. 1137-1145.

[3] M. Salazar K. Minakata, M. Reznikov, "Electrically Enhanced Condensation II: Effects of the Electrospray*," IEEE Trans. Industry Applications*, vol. 51, no. 2, 2015, pp. 1146-1152.

[4] A. E. K. Sundén, K. Støchkel, S. Panja, U. Kadhane, P. Hvelplund, S. B. Nielsen, H. Zettergren, B. Dynefors, and K. Hansen, "Heat capacities of freely evaporating charged water clusters," *J. Chem. Phys.*, vol. 130, 224308(7), 2009.

[5] F. Yu, "Modified Kelvin–Thomson equation considering ion-dipole interaction: Comparison with observed ion-clustering enthalpies and entropies," *J. Chem. Phys*., vol. 122, 084503, 2005.